ELSEVIER

Journal of Photochemistry and Photobiology A: Chemistry 103 (1997) 213–220

Journal of PHOTOCHEMISTRY AND PHOTOBIOLOGY A: CHEMISTRY

Substitutional photochemistry of Ru(η^6-mes)$_2^{2+}$ and Ru(η^6-mes)(CH$_3$CN)$_3^{2+}$ (mes = 1,3,5-trimethylbenzene)

Richard J. Lavallee, Charles Kutal *

Department of Chemistry, The University of Georgia, Athens, GA 30602 USA

Received 21 August 1996; accepted 17 October 1996

Abstract

Irradiation of Ru(η^6-mes)$_2^{2+}$ (mes is 1,3,5-trimethylbenzene, or mesitylene) in acetonitrile results in the substitution of one mesitylene ring by solvent to yield the half-sandwich complex, Ru(η^6-mes)(CH$_3$CN)$_3^{2+}$. The quantum efficiency of this process exhibits little dependence upon the excitation wavelength or the presence of oxygen, but varies with solvent in the order acetonitrile > water > acetone. Photolysis of Ru(η^6-mes)(CH$_3$CN)$_3^{2+}$ in acetonitrile occurs via two competing pathways: substitution of mesitylene by solvent to produce Ru(CH$_3$CN)$_6^{2+}$, and exchange of coordinated CH$_3$CN with bulk solvent. Quantum efficiencies for both pathways increase with decreasing excitation wavelength and, at each wavelength, CH$_3$CN exchange is more efficient than mesitylene substitution. Photochemical mechanisms for these processes are discussed and comparisons with related complexes are presented. © 1997 Elsevier Science S.A.

Keywords: Photochemistry; Photosubstitution; Ruthenium (II) complexes

1. Introduction

Members of the CpM(η^6-arene)$^+$ family (M is Fe or Ru, Cp is η^5-C$_5$H$_5$) undergo a variety of mechanistically interesting photochemical reactions in solution [1]. Early work by Mann and coworkers established that irradiation of these mixed-ring sandwich complexes leads to selective photosubstitution of the arene ligand by solvent or an added nucleophile (Eq. (1); L is a monodentate Lewis base) [2–5]. This reaction appears to originate from the lowest ligand field triplet state populated via efficient relaxation from higher-lying excited states. The quantum yield of arene substitution depends upon the electronic and steric properties of the carbocyclic rings and the nucleophilicity of the entering group, L. These characteristics support a mechanism in which L assists the displacement of the coordinated arene via nucleophilic attack on the excited metal center.

$$\mathrm{CpFe}(\eta^6-\mathrm{arene})^+ \xrightarrow[\mathrm{L}]{h\nu} \mathrm{CpFe(L)_3^+} + \mathrm{arene} \quad (1)$$

$$\mathrm{CpFe}(\eta^6-\mathrm{arene})^+ + \mathrm{hmdb} \xrightarrow{h\nu} \mathrm{CpFe}(\eta^6-\mathrm{hmb})^+ + \mathrm{arene} \quad (2)$$

In a later study, Roman et al. reported that several CpFe(η^6-arene)$^+$ complexes fluoresce in room-temperature dichloromethane [6]. Irradiation of the complexes in the presence of hexamethyl(Dewar benzene), hmbd, results in arene exchange accompanied by valence isomerization of hmdb to hexamethylbenzene, hmb (Eq. (2)). Luminescence characteristic of the product is observed under these conditions, thereby leading to the proposal that arene exchange and valence isomerization occur adiabatically on a singlet excited state surface without significant deactivation of the complex.

Replacing the cyclopentadienyl ring in CpFe(η^6-arene)$^+$ with a second arene yields complexes of the type M(η^6-arene)$_2^{2+}$. While the two families share common structural and electronic characteristics, they exhibit some clear differences in photochemical behavior. Lehmann and Kochi reported that irradiation into the ligand field bands of Fe(η^6-arene)$_2^{2+}$ results in the substitution of both arene ligands by solvent (Eq. (3)) [7]. Thus the absorption of a single photon triggers the release of two six-electron donor ligands without a change in the oxidation state of the metal. Our recent investigation of Fe(η^6-mes)$_2^{2+}$ (mes is 1,3,5-trimethylbenzene, commonly termed mesitylene) revealed that the quantum efficiency of this process varies from 0.6 to 1.0 over a range of excitation wavelengths that populates ligand field and mes → Fe charge-transfer excited states [8,9].

$$\mathrm{Fe}(\eta^6-\mathrm{arene})_2^{2+} \xrightarrow{h\nu} \mathrm{Fe}_{(\mathrm{solv})}^{2+} + 2\mathrm{arene} \quad (3)$$

* Corresponding author.

PII 1010-6030(96)04526-1

Interestingly, arene substitution occurs from both states, with each state following a different pathway to the common final products.

Continuing our investigation of bis(arene) metal complexes, we have turned our attention to the 4d congener, $Ru(\eta^6\text{-mes})_2^{2+}$. We report here that irradiation of this complex in acetonitrile initially causes the substitution of one mesitylene ligand by solvent to yield the half-sandwich product, $Ru(\eta^6\text{-mes})(CH_3CN)_3^{2+}$ (Eq. (4)). In a second, less efficient photochemical step, the remaining mesitylene is liberated to afford fully solvated Ru^{2+} (Eq. (5)).

$$Ru(\eta^6-mes)_2^{2+} \xrightarrow[CH_3CN]{h\nu} Ru(\eta^6-mes)(CH_3CN)_3^{2+} + mes \quad (4)$$

$$Ru(\eta^6-mes)(CH_3CN)_3^{2+} \xrightarrow[CH_3CN]{h\nu} Ru(CH_3CN)_6^{2+} + mes \quad (5)$$

Karlen et al. recently reported a study of the initial arene photosubstitution step for a series of bis(arene) Ru(II) complexes [10], while an earlier investigation by Weber and Ford focused upon photoinduced arene substitution in several $Ru(\eta^6\text{-arene})(H_2O)_n(NH_3)_{3-n}^{2+}$ ($n=0$, 1, or 3) complexes [11]. Our results complement this previous work by providing the first detailed characterization of both arene photosubstitution processes (Eqs. (4) and (5)) for a single complex. Moreover, we find that photoinduced loss of the monodentate ligands in the half-sandwich complex (Eq. (6); $n=1$–3) can occur with appreciably higher quantum efficiency than heretofore reported.

$$Ru(\eta^6-mes)(CH_3CN)_3^{2+} \xrightarrow[CD_3CN]{h\nu} Ru(\eta^6-mes)(CH_3CN)_{3-n}(CD_3CN)_n^{2+} \quad (6)$$

2. Experimental

2.1. Materials and syntheses

All chemicals were at least reagent grade quality and used as received from the supplier (Aldrich). Solvents were spectroscopic grade and used without further purification (Aldrich). Analytically pure $[Fe(\eta^6\text{-mes})_2](PF_6)_2$ was synthesized by a previously reported procedure [9]. $[Ru(\eta^6\text{-mes})_2](PF_6)_2$ was prepared by the Fischer–Hafner method [12]. Fresh $AlCl_3$, powdered Al, and $RuCl_3$ in deoxygenated mesitylene were heated at 80 °C for 3 h with stirring under a nitrogen atmosphere. The mixture was then cooled to 0 °C in an ice bath and deoxygenated H_2O was slowly added to hydrolyze any excess $AlCl_3$ and Al. The two-phase system was stirred, filtered into a separatory funnel, and the aqueous portion added dropwise to an aqueous solution of excess NH_4PF_6. The resulting precipitate was collected, washed with ether, and dried in vacuo. Purification was achieved by filtering an acetonitrile solution of the crude product through a 0.2 μm nylon filter, removing the solvent under vacuum, and repeatedly washing the off-white product with small amounts of acetonitrile. The air-stable, white microcrystalline powder was characterized by ^1H NMR and elemental analysis (Atlantic Microlab, Inc.). Calcd for $C_{18}H_{24}P_2F_{12}Ru$: C, 34.24; H, 3.83. Found: C, 34.21; H, 3.83.

$[Ru(\eta^6\text{-mes})(CH_3CN)_3](PF_6)_2$ was synthesized by a literature procedure [13], with the following modification. Previously prepared $[Ru(\eta^6\text{-mes})Cl_2]_2$ and exactly four equivalents of $AgNO_3$ were stirred in acetonitrile for 24 h at 35 °C. Solid AgCl was filtered off and the solvent removed by rotary evaporation. The yellow–orange solid was redissolved in a minimum of H_2O and added to an aqueous solution of excess NH_4PF_6, whereupon the product immediately precipitated. The yellow solid was redissolved in acetonitrile, filtered through a 0.2-μm nylon filter, and reprecipitated with diethyl ether. Further purification was achieved by slowly recrystallizing the product from acetonitrile–ether at 0 °C. The purity of the large yellow crystals was established by ^1H NMR and elemental analysis. Calcd for $C_{15}H_{21}N_3P_2F_{12}Ru$: C, 28.40; H, 3.34. Found: C, 28.46; H, 3.35.

2.2. Instrumentation

Electronic absorption spectra were recorded at room temperature on a Varian DMS 300 spectrophotometer. ^1H NMR spectra were recorded on a Bruker AC-250 spectrometer operating at 250.134 MHz. Chemical shifts were referenced to internal tetramethylsilane (TMS) by assigning the solvent peak a value of 1.95 ppm (CD_3CN), 2.04 ppm (CD_3COCD_3), or 4.80 ppm (D_2O). Relaxation delays of at least 20 s were employed between successive scans in order to achieve proper integrated signal areas.

High-pressure liquid chromatography (HPLC) experiments were performed on an apparatus consisting of an Alltech Associates model 425 pump, a Linear Instruments UV/Vis-200 absorbance detector operating at 230 nm, a Rheodyne sample injector with a 20-μL sample loop volume, and a Hamilton PRP-1 reversed-phase column (25×0.41 cm) with an associated Hamilton PRP-1 guard column. The mobile phase consisted of a 90:10 (v:v) mixture of acetonitrile–water, with 25 mM sodium hexanesulfonate and 20 mM triethylamine hydrochloride added as ion-interaction reagents. Chromatograms were recorded on a Hewlett–Packard 3396 Series II integrator. Previously constructed calibration curves were used to convert chromatographic peak areas to free mesitylene concentrations.

Conductivity measurements were performed on a Radiometer CDM80 conductivity meter equipped with a Type CDC114 cell with a cell constant of 0.97. Solutions were prepared in acetonitrile 2 h prior to measurement and shielded from room light at all times.

Photolyses at 313 nm and 365 nm were performed using an Illumination Industries, Inc. Model LH351P high-pressure mercury arc lamp situated 34 cm from the sample; the desired wavelengths were isolated by the use of a quartz-faced water filter and an appropriate narrow bandpass filter (width at half-height of 12 nm at 313 nm and either 25 or 31 nm at 365 nm). Experiments at 254 nm employed the direct output of an Ultra-violet Products, Inc. Pen-Ray lamp situated 2 cm from the sample. Light intensities in all cases were determined by potassium ferrioxalate actinometry [14].

2.3. Quantum yield measurements

Solutions of $Ru(\eta^6\text{-mes})_2^{2+}$ and $Ru(\eta^6\text{-mes})(CH_3CN)_3^{2+}$ were photolyzed in either 1.0-cm or 1.0-mm pathlength cells maintained at 21.0 ± 0.5°C in a thermostatted cell holder. Samples irradiated in 1.0 cm pathlength cells were magnetically stirred during photolysis, while samples in 1.0 mm cells were periodically removed from the light beam and shaken by hand. Typical initial concentrations were $4\text{–}6 \times 10^{-3}$ M. Deoxygenated samples were prepared by bubbling the solutions with argon for 30 min. Samples were irradiated to less than 20 percent reaction for most determinations of quantum yields. Corrections for inner filter effects were applied when necessary.

The extent of photolysis of $Ru(\eta^6\text{-mes})_2^{2+}$ (Eq. (4)) in acetonitrile was quantified spectrophotometrically by monitoring the increase in solution absorbance at 400 nm, a wavelength at which $Ru(\eta^6\text{-mes})_2^{2+}$ and $Ru(\eta^6\text{-mes})(CH_3CN)_3^{2+}$ have extinction coefficients of 4.5 and 360 $M^{-1}\,cm^{-1}$, respectively. Quantum yields calculated in this manner were confirmed by two independent methods. ^1H NMR spectroscopy was used to determine the concentration of unphotolyzed material by comparing the area of the ring proton signal of $Ru(\eta^6\text{-mes})_2^{2+}$ to the total ring proton area. Alternatively, the concentration of free mesitylene in photolyzed samples was measured by HPLC. The extent of photolysis of $Ru(\eta^6\text{-mes})_2^{2+}$ in water and acetone was followed by ^1H NMR.

Photoinduced deligation of mesitylene from $Ru(\eta^6\text{-mes})(CH_3CN)_3^{2+}$ (Eq. (5)) was monitored by ^1H NMR in a manner analogous to that for $Ru(\eta^6\text{-mes})_2^{2+}$. Exchange of coordinated and bulk acetonitrile (Eq. (6)) occurred both thermally and photochemically; each process was quantified by ^1H NMR by measuring the decrease in the signal area of coordinated CH_3CN. Thermal exchange obeyed first-order kinetics over at least four half-lives; the rate constant for this process was used to calculate the thermal correction applied to each irradiated sample.

3. Results and discussion

3.1. Spectroscopy and photochemistry of $Ru(\eta^6\text{-mes})_2^{2+}$

The electronic absorption spectrum of $Ru(\eta^6\text{-mes})_2^{2+}$ in room-temperature acetonitrile is shown in Fig. 1. We assign the three features appearing at 347 (sh), 296, and 254 (sh) nm as spin-allowed ligand field transitions of the low-spin, d^6 metal. In D_{3h} symmetry (eclipsed arrangement of the mesitylene rings), the state assignments in order of increasing energy are $a^1E'' \leftarrow {}^1A_1'$, $^1A_1''$, $^1A_2'' \leftarrow {}^1A_1'$, and $b^1E'' \leftarrow {}^1A_1'$, where we have assumed that the splitting of the A_1'' and A_2'' levels is too small to detect [15]. These transitions are blue-shifted approximately 10 kK relative to their counterparts in $Fe(\eta^6\text{-mes})_2^{2+}$ [9]; by comparison, the ligand field transitions in $CpRu(\eta^6\text{-mes})^+$ lie some 8 kK higher in energy than those in $CpFe(\eta^6\text{-mes})^+$ [4]. The spectrum of $Ru(\eta^6\text{-mes})_2^{2+}$ also contains a shoulder at 232 nm that lies on the tail of an intense absorption extending below 200 nm. Possible assignments of either feature are a metal–ligand charge transfer (Ru → mes or mes → Ru) transition or a π–π^* transition localized on the mesitylene ring. Surprisingly, no feature clearly attributable to the spin-forbidden $a^3E'' \leftarrow {}^1A_1'$ ligand field transition is discernible out to 600 nm.

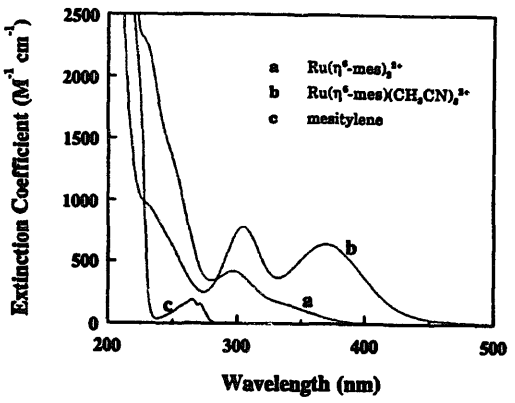

Fig. 1. Electronic absorption spectra in acetonitrile of (a) $Ru(\eta^6\text{-mes})_2^{2+}$, (b) $Ru(\eta^6\text{-mes})(CH_3CN)_3^{2+}$, and (c) mesitylene.

Continuous photolysis at 313 nm causes an initially colorless solution of $Ru(\eta^6\text{-mes})_2^{2+}$ in acetonitrile to turn yellow. Fig. 2 illustrates the photoinduced growth of two bands in the long-wavelength region and the appearance of isosbestic points at 273 and 284 nm. Identical spectral changes occur upon photolysis at 254 nm, 365 nm, and with Pyrex-filtered light ($\lambda > 290$ nm). The photoreactions are irreversible and the photoproducts are thermally stable for up to three weeks at room temperature. Extensive photolysis produces a

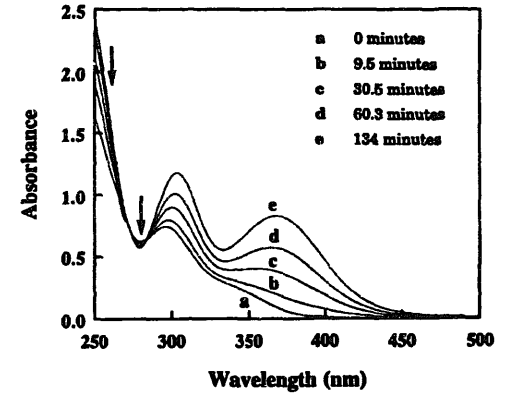

Fig. 2. Electronic spectral changes resulting from the 313-nm irradiation of $Ru(\eta^6\text{-mes})_2^{2+}$ in acetonitrile; a–e indicate irradiation times.

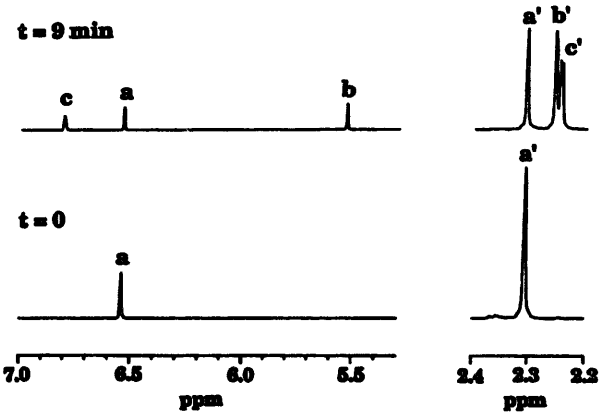

Fig. 3. NMR spectral changes resulting from photolysis of $Ru(\eta^6\text{-mes})_2^{2+}$ in CD_3CN. Spectra taken before ($t=0$) and after ($t=9$ min) irradiating the sample in an NMR tube with white light ($\lambda>290$ nm). Peak labels: a identifies the ring protons and a' the methyl protons in $Ru(\eta^6\text{-mes})_2^{2+}$, while b,b' and c,c' refer to the corresponding protons in $Ru(\eta^6\text{-mes})(CD_3CN)_3^{2+}$ and mesitylene, respectively.

diminution in the intensities of the long-wavelength bands and the growth of new bands at about 320 and 265 nm, the latter feature exhibiting fine structure characteristic of the mesitylene chromophore. These long-photolysis results are consistent with the ultimate production of $Ru(CH_3CN)_6^{2+}$ [16] and free mesitylene [17].

Further identification of the photoproducts was accomplished by ^1H NMR spectroscopy (Fig. 3). Acetonitrile-d_3 solutions of $Ru(\eta^6\text{-mes})_2^{2+}$ exhibit two singlets at 2.31 and 6.54 ppm which are assigned to the methyl and ring protons, respectively, of the mesitylene ligands. Samples are stable at room temperature for up to three weeks in the dark. Irradiation causes new resonances to appear at 2.26 ppm (singlet), 5.53 ppm (singlet), 2.25 ppm (doublet, $^4J_{HH}=0.87$ Hz), and 6.80 ppm (unresolved multiplet). By comparison to the spectra of authentic samples, we can assign the first two signals to the methyl and ring protons, respectively, of coordinated mesitylene in $Ru(\eta^6\text{-mes})(CD_3CN)_3^{2+}$, and the last two signals to the corresponding protons of free mesitylene. The methyl signals of the two photoproducts partially overlap and could not be completely resolved. Therefore, quantitative information regarding the relative concentrations of these photoproducts was obtained from the integrated areas of the mesitylene ring protons. Table 1 lists the percentage contributions of $Ru(\eta^6\text{-mes})_2^{2+}$, $Ru(\eta^6\text{-mes})(CD_3CN)_3^{2+}$, and free mesitylene to the total ring proton area as function of irradiation time. These data indicate that photolysis of the parent complex yields the two photoproducts in a one-to-one ratio. This stoichiometry persists to about 90% conversion, whereupon the concentration of free mesitylene begins to increase more rapidly than that of $Ru(\eta^6\text{-mes})(CD_3CN)_3^{2+}$. Following complete reaction of $Ru(\eta^6\text{-mes})_2^{2+}$, further irradiation causes the continued production of mesitylene and the accompanying disappearance of the half-sandwich complex. Collectively, these NMR results and the electronic spectral changes described earlier (Fig. 2) establish that arene

Table 1
Relative concentrations of $Ru(\eta^6\text{-mes})_2^{2+}$ and two photoproducts in acetonitrile solution as a function of irradiation time

Irradiation time (/min)	% $Ru(\eta^6\text{-mes})_2^{2+}$	% Mesitylene	% $Ru(\eta^6\text{-mes})(CD_3CN)_3^{2+}$
0	100	0	0
14	24	37	38
22	16	41	43
31	12	43	45
56	8	47	45
90	1	52	47
253	0	60	40
1182	0	88	12

photosubstitution occurs sequentially according to Eqs. (4) and (5).

Table 2 contains a summary of quantum yield (Φ_1) data for the first substitution step measured under a variety of experimental conditions. These results reveal that Φ_1 has little or no dependence upon the excitation wavelength (compare runs 1, 7, 12 or 4, 10, 14), perdeuteration of the solvent (runs 1, 3 or 7, 8), and the presence of oxygen (runs 1, 2 or 13, 15). In contrast, Φ_1 varies markedly upon changing solvents in the order acetonitrile > water > acetone (runs 4, 6, 17).

Acetonitrile solutions of $[Fe(\eta^6\text{-mes})_2](PF_6)_2$ yield a linear plot of molar conductance against the square root of concentration (correlation coefficient = 0.996) over the range $1.0\text{–}5.0\times10^{-3}$ M. Such behavior indicates that ion-pair

Table 2
Photosubstitution quantum yields for $Ru(\eta^6\text{-mes})_2^{2+}$

Run	λ_{excit} (/nm)	Solvent	Ar purged	Analysis[a]	Φ_1[b]
1	254	CD_3CN	No	Vis	0.13 ± 0.01 (5)
2	254	CD_3CN	Yes	Vis	0.15 (1)
3	254	CH_3CN	No	Vis	0.15 ± 0.00 (3)
4	254	CD_3CN	No	NMR	0.12 ± 0.00 (5)
5	254	CD_3CN	Yes	NMR	0.11 (1)
6	254	D_2O	No	NMR	0.0036 ± 0.0005 (3)
7	313	CD_3CN	No	Vis	0.16 ± 0.00 (3)
8	313	CH_3CN	No	Vis	0.16 ± 0.00 (3)
9	313	CH_3CN	Yes	Vis	0.16 ± 0.00 (2)
10	313	CD_3CN	No	NMR	0.13 ± 0.04 (4)
11	313	CH_3CN	No	HPLC	0.16 ± 0.00 (2)
12	365	CD_3CN	No	Vis	0.12 (1)
13	365	CH_3CN	No	Vis	0.12 ± 0.02 (4)
14	365	CD_3CN	No	NMR	0.13 (1)
15	365	CH_3CN	Yes	Vis	0.13 (1)
16	365	CH_3CN[c]	No	Vis	0.12 (1)
17	365	$(CD_3)_2CO$	No	NMR	0.0011 (1)

[a] Analytical technique employed to determine the extent of photolysis (see Section 2).

[b] Quantum yield for substitution of one mesitylene by solvent. Error limits represent deviation from the mean for two or more runs; number of runs indicated in parentheses. We estimate the accuracy of the quantum yields to be ±10–15% for the vis and HPLC measurements, and ±20–30% for the NMR measurements.

[c] Solution contains 1.2×10^{-2} M NH_4PF_6.

formation between Fe(η^6-mes)$_2^{2+}$ and PF_6^- is unimportant in this concentration regime. Since ion pairing should be less favorable for the larger Ru(η^6-mes)$_2^{2+}$, we conclude that ion pairs do not play a significant role in the photochemistry of this complex in CH_3CN or the more polar solvent H_2O. The insensitivity of Φ_1 to the presence of excess PF_6^- (Table 2, runs 13, 16) supports this conclusion.

3.2. Spectroscopy and photochemistry of Ru(η^6-mes)(CH$_3$CN)$_3^{2+}$

Attempts to obtain a pure sample of Ru(η^6-mes)-(CH$_3$CN)$_3^{2+}$ as the PF_6^- salt by irradiating [Ru(η^6-mes)$_2$](PF$_6$)$_2$ in acetonitrile proved unsuccessful. This procedure involved extensive photolysis of the starting complex until no further absorbance increases in the long-wavelength bands (Fig. 2) were observed, followed by removal of solvent and free mesitylene under vacuum. The integrated area of coordinated acetonitrile ($\delta = 2.51$ ppm) in the NMR spectrum of the isolated solid was greater than expected, thus suggesting the production of Ru(CH$_3$CN)$_6^{2+}$ by secondary photolysis of Ru(η^6-mes)(CH$_3$CN)$_3^{2+}$ (Eq. (5)). A subsequent study of the photoproducts as a function of irradiation time (Table 1) confirmed that conversion of Ru(η^6-mes)$_2^{2+}$ to Ru(η^6-mes)(CH$_3$CN)$_3^{2+}$ is incomplete before this second photochemical process begins. Consequently, the half-sandwich complex was synthesized and characterized independently.

Fig. 1 depicts the electronic absorption spectrum of Ru(η^6-mes)(CH$_3$CN)$_3^{2+}$ in room-temperature acetonitrile. By analogy to the spectral assignments offered by Weber and Ford for several Ru(η^6-arene)(H$_2$O)$_n$(NH$_3$)$_{3-n}^{2+}$ complexes [11], we assign the features appearing at 369, 304 and 234 (sh) nm as spin-allowed ligand field transitions. A first-derivative analysis of the spectrum suggests the presence of a shoulder at 254 nm, which may correspond to the fourth ligand field transition expected in a complex with C_{3v} symmetry. A shoulder at 209 nm (not shown in Fig. 1) appears on the intense absorption that extends below 200 nm. These high-energy features most likely arise from charge transfer and/or intraligand transitions.

Irradiation of Ru(η^6-mes)(CH$_3$CN)$_3^{2+}$ in acetonitrile results in the substitution of mesitylene by solvent (Eq. (5)). Table 3 contains a summary of quantum yield (Φ_2) data for this reaction at various excitation wavelengths. Values of Φ_2 are significantly lower than the Φ_1 values found for Ru(η^6-mes)$_2^{2+}$ (Table 2), but are comparable to the quantum yields reported for arene substitution in a series of Ru(η^6-arene)(H$_2$O)$_n$(NH$_3$)$_{3-n}^{2+}$ complexes [11]. The steady increase of Φ_2 at shorter wavelengths mirrors the behavior seen in this earlier study.

In the course of characterizing Ru(η^6-mes)(CH$_3$CN)$_3^{2+}$ by NMR spectroscopy, we noticed the progressive reduction in the area of the resonance for coordinated CH$_3$CN and the concomitant appearance of a signal ($\delta = 1.974$ ppm) characteristic of free CH$_3$CN. This behavior indicates that bound

Table 3
Photosubstitution quantum yields for Ru(η^6-mes)(CH$_3$CN)$_3^{2+}$ in acetonitrile [a]

λ_{excit} (/nm)	$\Phi_2^{a,c}$	$\Phi_3^{b,c}$	Φ_3/Φ_2
254	0.0024 ± 0.0002 (2)	0.47 ± 0.10 (3)	200 ± 60
313	0.0011 ± 0.0003 (3)	0.42 ± 0.08 (3)	380 ± 180
365	0.00031 ± 0.00001 (2)	0.22 ± 0.01 (2)	710 ± 55

[a] Quantum yield for substitution of mesitylene according to Eq. (5).
[b] Quantum yield for exchange of coordinated and bulk acetonitrile according to Eq. (6).
[c] Error limits represent deviation from the mean of two or more runs; number of runs indicated in parentheses. We estimate the accuracy of the quantum yields to be ±20–30%.

CH$_3$CN can undergo exchange with the bulk deuterated solvent (Eq. (6)). Interestingly, irradiation accelerates this process, and values of the quantum yield (Φ_3) of photochemical exchange at different excitation wavelengths are listed in Table 3. These values have been corrected for the accompanying thermal ligand exchange, which occurs with a pseudo first-order rate constant of $3.6 \pm 0.2 \times 10^{-5}$ s^{-1} at 21.0 ± 1.0 °C.

3.3. Mechanistic considerations

Irradiation of Ru(η^6-mes)$_2^{2+}$ in acetonitrile causes the substitution of one mesitylene ring by solvent (Eq. (4)). The wavelengths employed (254, 313, and 365 nm) excite the spin-allowed ligand field transitions of the complex with some contribution (particularly at 254 nm) from π–π^* and/or charge transfer transitions. The absence of a significant wavelength dependence of the quantum yield (Table 2) implies that either the reaction occurs with comparable efficiencies from two (or more) excited states, or that higher-lying excited states relax with comparable efficiencies to a common reactive state. The latter possibility appears to be more realistic, and thus we propose that arene substitution originates from the lowest ligand field excited state, a^1E'', or its triplet counterpart, a^3E''. Both states arise from the one-electron transition between a molecular orbital that is essentially metal $4d_z^2$ in character and nonbonding, and a higher-energy, predominantly metal-centered molecular orbital that is antibonding with respect to the metal-ligand bonds [10]. The redistribution of electron density which accompanies this transition weakens the Ru–mes bonding and creates an energetically low-lying vacancy in the $4d_z^2$ orbital that enhances the susceptibility of the metal to nucleophilic attack by the solvent.

Once populated, the reactive aE'' state (we ignore spin labels in the remaining discussion) can undergo deactivation to the ground state in competition with nucleophilic addition of a solvent molecule to form an intermediate, I, containing an η^4-bonded mesitylene ring (Scheme 1; S is CH$_3$CN). This intermediate, in turn, has the option of reacting further with solvent to yield Ru(η^6-mes)(CH$_3$CN)$_3^{2+}$ or expelling coordinated solvent to regenerate the parent complex. We attribute

the marked solvent dependence of the photosubstitution quantum yield (Table 2) to the varying abilities of different solvents to compete with the labilized arene ligand for coordination sites about the metal. Strongly coordinating solvents should favor the formation and further reaction of I and thereby increase the value of Φ_1. Acetonitrile serves as a particularly effective solvent for displacing mesitylene from Ru(II); this property undoubtedly reflects the high stability of the Ru–$NCCH_3$ bond that results from the back-donation of electron density from the metal to the low-lying π^* orbitals on the ligand [18].

The present study of the photosubstitutional chemistry of Ru(η^6-mes)$_2^{2+}$ has yielded results that agree in most respects with those reported by Karlen et al. for a series of related bis(arene) Ru(II) complexes [10]. Mention should be made, however, of one important difference. In contradistinction to data in Table 2 (e.g. runs 1, 7, 12), the earlier workers observed a marked wavelength dependence of the quantum yield of initial arene loss. We can offer no explanation for this disparity, but simply note that different solvent systems were employed in the two studies: acetonitrile and water (0.05 M H_2SO_4)–ethanol (3:2).

Irradiation into the ligand field absorption bands of Ru(η^6-mes)$(CH_3CN)_3^{2+}$ in acetonitrile causes the substitution of the arene ligand by solvent (Eq. (5)). This behavior has precedent in the work of Weber and Ford [11], who reported that several Ru(η^6-arene)$(H_2O)_n(NH_3)_{3-n}^{2+}$ complexes follow a similar pathway in aqueous solution. Quite unexpected, however, is the observation that Ru(η^6-mes)$(CH_3CN)_3^{2+}$ undergoes efficient photochemical exchange of coordinated CH_3CN with the bulk solvent (Eq. (6)). By comparison, negligible photolabilization of monodentate ligands ($\Phi_{NH_3} < 5 \times 10^{-4}$) was observed for Ru($\eta^6$-$C_6H_6$)$(NH_3)_3^{2+}$ and Ru(η^6-C_6H_6)$(H_2O)(NH_3)_2^{2+}$ in the earlier study [11]. Several factors could contribute to this striking disparity in the quantum yields of monodentate ligand substitution: these include the use of different arenes (benzene rather than mesitylene), monodentate ligands (σ-bonding NH_3 rather than σ-bonding and π-backbonding CH_3CN), and solvents (H_2O rather than CH_3CN). Further studies are needed to assess the relative importance of each factor.

Both photosubstitution reactions of Ru(η^6-mes)-$(CH_3CN)_3^{2+}$ exhibit wavelength-dependent quantum yields (Table 3). One explanation for such behavior is that each of the reactions originates from two (or more) excited states, with the higher-energy state(s) being the more reactive. Alternatively, both reactions could originate from a single, nonspectroscopic state that is populated with increasing efficiency from higher-lying states. The quantum yield ratio, Φ_3/Φ_2, affords a means of distinguishing between these two explanations; thus, a single reactive state requires a constant ratio as a function of excitation wavelength, whereas multiple reactive states can accommodate a variable ratio. Despite rather large error limits, the data in Table 3 reveal a trend in Φ_3/Φ_2 toward smaller values at shorter wavelengths. This result supports the involvement of at least two reactive excited states in the substitutional photochemistry of Ru(η^6-mes)$(CH_3CN)_3^{2+}$.

Scheme 2 depicts a proposed mechanism that accounts for the observed photoproducts (S is CH_3CN, S′ is CD_3CN). Arene substitution proceeds by way of a photogenerated η^4-bonded intermediate, II, which has the option of reacting further with solvent to yield fully solvated Ru^{2+} or expelling

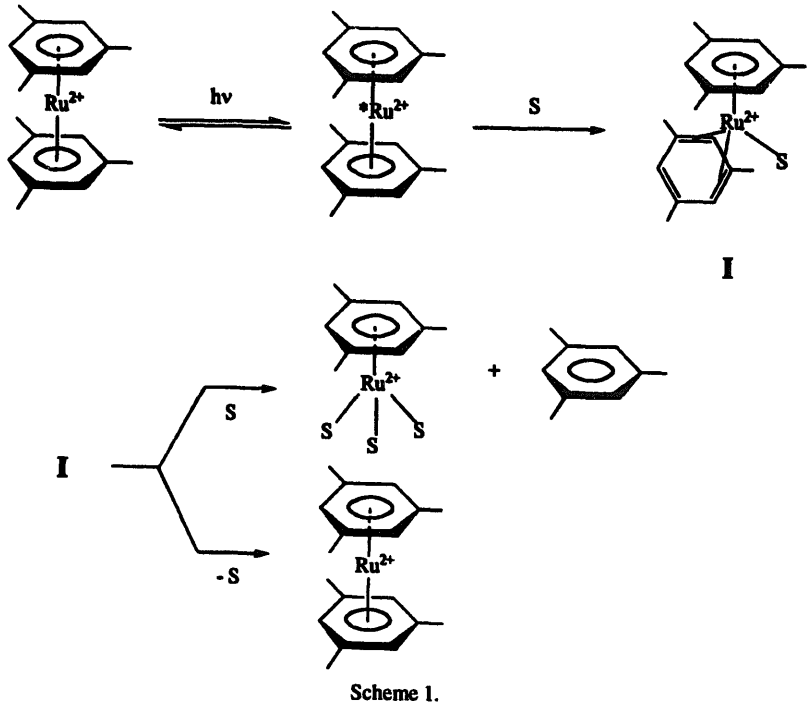

Scheme 1.

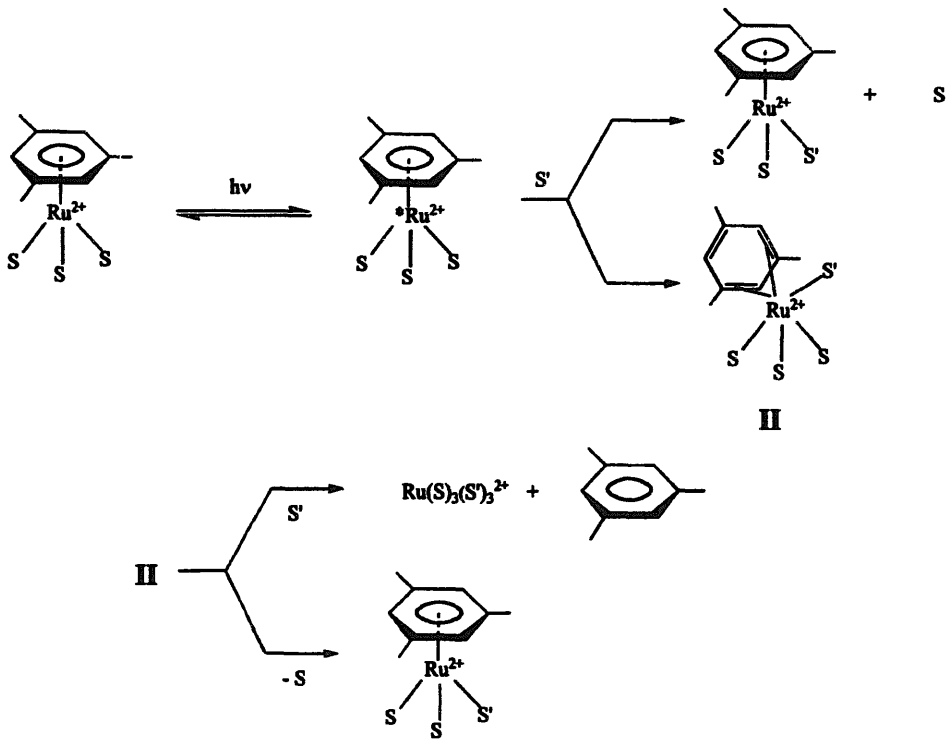

Scheme 2.

a coordinated solvent molecule to reform the mono(arene) complex. Note that the latter option provides a pathway for acetonitrile exchange. Alternatively, exchange may occur directly from an excited state without the involvement of II.

4. Concluding remarks

The sequential photosubstitution of the arene ligands in $Ru(\eta^6\text{-mes})_2^{2+}$ (Eqs. (4) and (5)) provides an interesting contrast to the behavior of its 3d congener $Fe(\eta^6\text{-mes})_2^{2+}$, which loses both arenes upon the absorption of a single photon (Eq. (3)) [8,9]. These different pathways for arene deligation reflect the different thermal stabilities of the half-sandwich complexes formed in the initial photochemical step. Thus, while $Fe(\eta^6\text{-mes})(CH_3CN)_3^{2+}$ undergoes very rapid (within a few microseconds [9]) thermal substitution of mesitylene by solvent at room temperature to yield $Fe(CH_3CN)_6^{2+}$, the thermally robust $Ru(\eta^6\text{-mes})(CH_3CN)_3^{2+}$ requires photoactivation to produce $Ru(CH_3CN)_6^{2+}$. A similar difference in thermal stabilities exists for the pair of half-sandwich complexes, $CpFe(CH_3CN)_3^{+}$ and $CpRu(CH_3CN)_3^{+}$ [5].

Practical interest in cationic arene complexes of Fe(II) and Ru(II) has grown in recent years owing to their utility as photochemical synthons [19,20], photoinitiators [21], and photocatalysts [16]. The present study has delineated the rich solution photochemistry of one member of the bis(arene) Ru(II) family. Future work will explore the efficacy of $Ru(\eta^6\text{-mes})_2^{2+}$ as a cationic photoinitiator for the crosslinking and photoimaging of epoxide-functionalized polymer films.

Acknowledgements

We thank Dr Gary Gamble for performing some preliminary experiments and Professor A. Ludi for providing the absorption spectrum of $Ru(CH_3CN)_6^{2+}$. Financial support for this work was received from the National Science Foundation (Grant DMR-9122653).

References

[1] K.R. Mann, A.M. Blough, J.L. Schrenk, R.S. Koefod, D.A. Freedman and J.R. Matachek, *Pure Appl. Chem., 67* (1995) 95.
[2] T.P. Gill and K.R. Mann, *Inorg. Chem., 19* (1980) 3007.
[3] J.L. Schrenk, M.C. Palazzotto and K.R. Mann, *Inorg. Chem., 22* (1983) 4047.
[4] A.M. McNair, J.L. Schrenk and K.R. Mann, *Inorg. Chem., 23* (1984) 2633.
[5] J.L. Schrenk, A.M. McNair, F.B. McCormick and K.R. Mann, *Inorg. Chem., 25* (1986) 3501.
[6] E. Roman, M. Barrera, S. Hernandez and E. Lissi, *J. Chem. Soc., Perkin Trans. II* (1988) 939.
[7] R.E. Lehman and J.K. Kochi, *J. Am. Chem. Soc., 113* (1991) 501.
[8] G. Gamble and C. Kutal, *Polym. Adv. Technol., 5* (1994) 63.
[9] G. Gamble, P.A. Grutsch, G. Ferraudi and C. Kutal, *Inorg. Chim. Acta, 247* (1996) 5.
[10] T. Karlen, A. Hauser and A. Ludi, *Inorg. Chem., 33* (1994) 2213.
[11] W. Weber and P.C. Ford, *Inorg. Chem., 25* (1986) 1088.
[12] V.E.O. Fischer and R. Bottcher, *Z. Anorg. Allg. Chem., 291* (1957) 303.

[13] M.A. Bennett and A.K. Smith, *J. Chem. Soc., Dalton Trans.* (1974) 233.
[14] C.G. Hatchard and C.A. Parker, *Proc. R. Soc. London, Ser. A, 235* (1956) 518.
[15] Y.S. Sohn, D.N. Hendrickson and H.B. Gray, *J. Am. Chem. Soc., 93* (1971) 3603.
[16] T. Karlen, A. Ludi, A. Muhlebach, P. Bernhard and C. Pharisa, *J. Polym. Sci. Part A, 33* (1995) 1665.
[17] F. Dorr and G. Buttgereit, *Ber. Bunsenges. Phys. Chem., 67* (1963) 867.
[18] I. Rapaport, L. Helm, A.E. Merbach, P. Bernhard and A. Ludi, *Inorg. Chem., 27* (1988) 873.
[19] A.M. McNair and K.R. Mann, *Inorg. Chem., 25* (1986) 2519.
[20] J. Ruiz, M.A. Gonzalez, E. Roman and M.T. Garland, *J. Chem. Soc. Dalton Trans.* (1990) 21.
[21] R. Bowser and R.S. Davidson, *J. Photochem. Photobiol. A: Chem., 77* (1994) 269.